GEOLOGICAL AND GEOCHEMICAL INVESTIGATIONS ON HAMMAMAT MOLASSE SEDIMENTS, G. KHARAZA, EASTERN DESERT, EGYPT

Said.A. Azzaz[1], Sherif Kharbish[2]* and Hesham. M. El-alfy[1]

[1]Said.A. Azzaz, Hesham. M. El-alfy, Geology department, Faculty of Science, Zagazig University, Zagazig, Egypt

[2]Sherif Kharbish, Department, Faculty of Science, Suez University, Suez 43518, Egypt

*corresponding author e-mail:

sherifkharbish@hotmail.com, sherif.abdalla@suezuniv.edu.egt ,

Abstract: The Hammamat molasse sediments of the Eastern Desert of Egypt were deposited in isolated basins formed during an initial stage of orogen parallel N–S extension (650–580 Ma) in the Neoproterozoic time. Supply of sediments to the molasse basins began after the eruption of Dokhan volcanics (602–593 Ma), the present study basin is one of several Pan-African, sedimentary basins formed across several hundreds of kilometres of the Eastern Desert of Egypt. It comprises two stages of sedimentation: The earlier stage is characterised by the deposition of fluviatile sediments and later influx of granitic clasts indicating that this part of the basin formed mostly after intrusion of what is known as the ‘‘older’’ granite generation in the Eastern Desert around 650–610 Ma. Geochemical studies revealed that the Hammamat sedimentary rocks were originated from felsic and intermediate igneous sources. Also, these rocks were probably formed in a continental arc setting.

Key words: Hammamat molasse sediments, Eastern Desert of Egypt, Geochemistry

Introduction

The Hammamat Group (HG) is a sequence of immature, clastic sedimentary rocks that crop out sporadically throughout the central and northern segments of the Eastern Desert of Egypt. It is represented by clastic sediments attaining a thickness of about 4000 m (Akkad and Noweir, 1980) at its type locality Wadi Hammamat, CED, Egypt (Hassan and Hashad, 1990).

HG is texturally immature (El Kalioubi, 1996) and was considered to reflect a significant change in Pan-African tectonics in the Eastern Desert, marking the end of a compressive, subduction-related regime and the onset of extension (Stern and Hedge, 1985). In the ED, HG was subdivided into Lower Igla Formation is a sequence of interbedded red to purple colored sandstones, siltstones and conglomerates. Upper Shihimiya Formation is composed of green to grey conglomerates, greywacke and siltstones by Akkad and Noweir (1980). Whereas, Willis et al. (1988) divided HG into lower series composed mainly of polymictic breccia and the upper series, which is composed of sandstone and shale.

Hammamat Sediments (HS) are generally unmetamorphosed (Akkad and Noweir, 1980) and were considered as the erosion products from pen-contemporaneous Dokhan Volcanics that were accumulated in intermontane and foreland basins (El Gaby et al., 1990). They might have been deposited in two stages; the first stage marks the closure of the ocean basin and the deposition of the sediments along convergent margin, whereas the second one marks the advanced stage of the collision, and the deposition in inter-montane basins away from the collision zone (Shalaby et al., 2006).

Methodology

Eleven representative samples of the present rock suite were collected for petrographical and geochemical investigations. The petrographical investigations were done using the Nikon (Optiphoto-Pol) polarizing microscope, equipped with an automatic photomicrographic apparatus (Microflex AFX-П). All of samples were subjected to XRF analyses.Whole rock geochemical analyses were carried out for major elements using wet chemical analysis techniques (Shapiro and Brannock, 1962). The trace elements were analyzed using XRF technique (Philips pw 1410 together with a Mo-target tube operated at 50kv and 30 mA). All analyses were carried out in the laboratories of the Nuclear Materials Authority (N.M.A), Egypt.

Geological setting and Petrographical investigation of Gebel El Kharaza area

Gebel El Kharaza area (27° 51` 30" – 27° 55` 40" N and – 32° 48` 50" – 32° 52` 40" E) is located in the northern part of the Eastern Desert of Egypt. It comprises Late Proterozoic Dokhan volcanic rocks, Hammamat sediments (HS) together with Old and Young Granitoids as well as few outcrops of Metavolcanics (Fig 1).

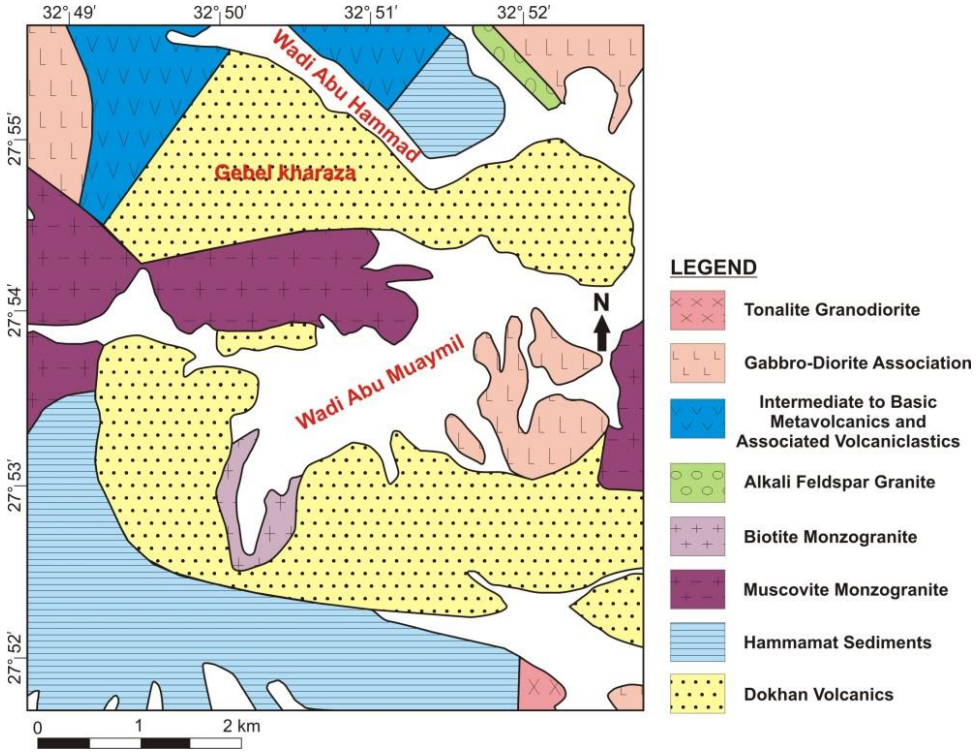

Fig 1 Geological map of G. Kharaza area

The occurrence of the HS in the study area is extremely involved close to the outcrops of the Dokhan volcanics. Occasionally, they are less dominant than Dokhan volcanics occupying relatively small areas at the slopes and flanks with low to moderate mountainous terrain (Fig 2a). They comprise interbedded succession of purple, brick, red and gray to grayish green siltstones and sandstones (Fig 2b), associated together with a distinctive polymictic conglomeratic facies (Fig 2c). HS are usually massive, undeformed, locally associated with foliated varieties. They are intruded by Older granite (Fig 2d), Younger monzogranite, with minor sheets or dykes of felsite and quartz-feldspar porphyry. They can be easily distinguished from the surrounding rocks by their distinct bedding. Bedding is expressed in the alternation of conglomerate beds with greywacke and siltstone beds, where the bedding plane of these sediments is variably trending with gentle to moderate dips. Local horizontal and sub-horizontal beds are recorded in the study area (Fig 2e).

A basal conglomerate bed is identified including pebbles, boulders and cobbles of Dokhan volcanics together with different composition of granites, granodiorites, monzogranite and alkali feldspar granites. They include variable proportion with different sizes and shapes of crystal fragments (quartz and feldspar) and local abundance of rock fragments. The rock fragments are composed mainly of volcanics, dyke rocks, granites, felsites and immature sediments with shades of pink, gray, green and black, which are embedded in a fine grained argillaceous cement and/or purple red hematitic clayey matrix. The conglomerates are relatively poorly sorted, have sub-rounded to well rounded or ellipsoidal polymictic boulders, cobbles and pebbles reaching up to 80 cm across. But the common size ranges between 7-10 cm. Microscopically, the crystal fragments are quartz, plagioclase and epidote. Quartz clasts are common, corroded by the matrix (Fig 3a), while plagioclase and k-feldspar fragments are usually altered to loose their identity. Sometimes, the alteration of the large crystal fragments is less than the smaller ones and can show the lameller and simple twinning (Fig 3b). The rock fragments are amygdaloidal – porohyritic andesite, dacite, rhyodacite, tuffs (Fig 3b), hematitized volcanic glass and granites as well as reworked Hammamat sedimentary rocks. Matrix is occasionally foliated and stretched around the pebbles.

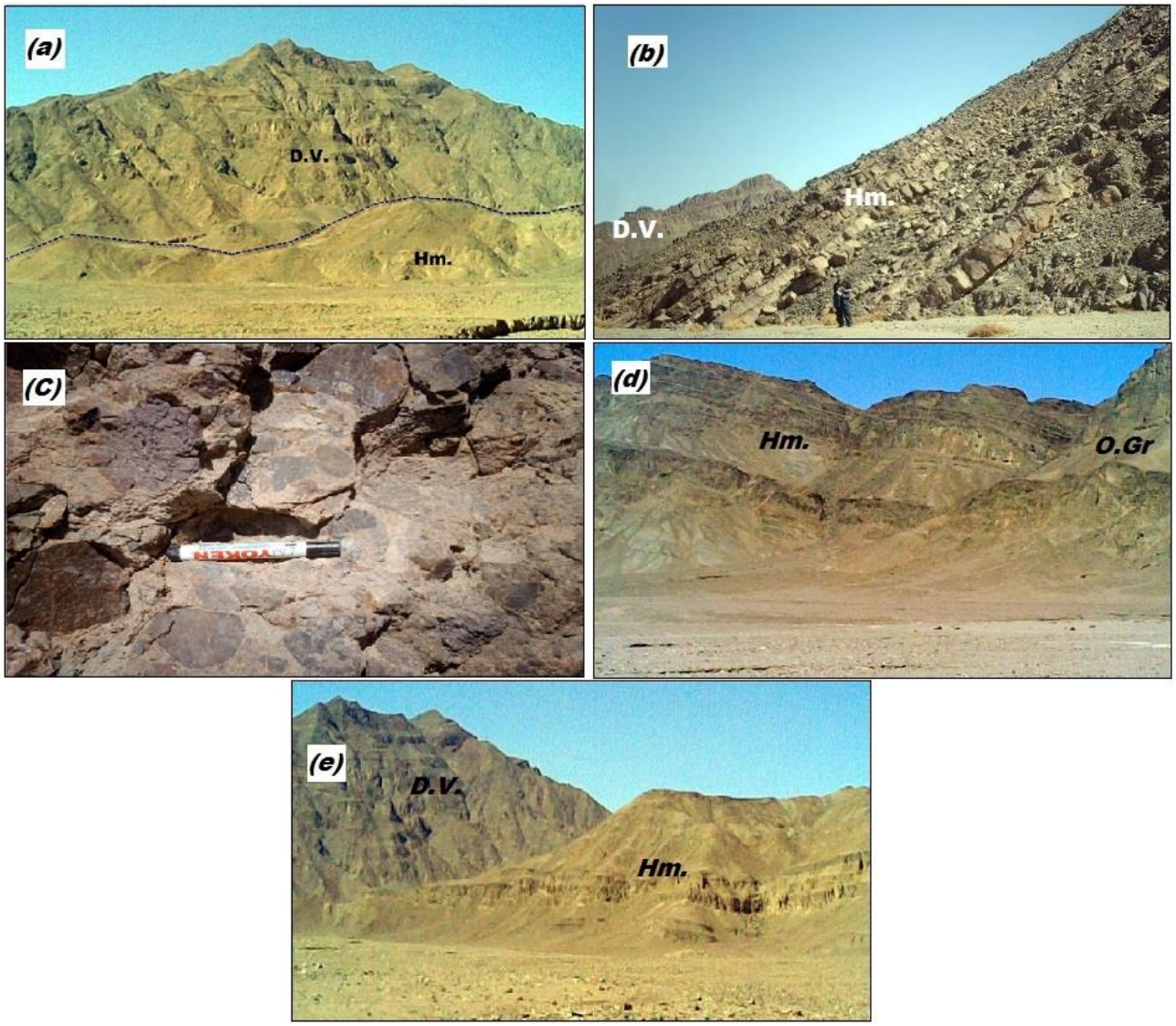

Fig 2 (a) Panoramic view of a thick sequence of Gabal Kharaza Dokhan volcanics, and appearance of low hills of Hammamat sediments at its foot (looking S.), (b) Interbedded succession of siltstones and sandstones of the Hammamat sediments, entrance of Wadi Abu Hammad (looking N.), (c) Pebbles and cobbles of volcanic and granitic composition in a conglomeratic Hammamat bed, mouth of W.Abu Hammad (looking W), (d) Sharp intrusive contact between Hammamat sediments (Hm.) and older granite (O.Gr) south G.Kharaza. (looking W.), (e) Panoramic view of sub-horizontal beds of Hammamat sediments (Hm.) followed by Kharaza Dokhan volcanics (D.V.) at the entrance of Wadi Abu Hammad. (looking SW)

Sandstones (greywackes) are fine to medium grained with local grading into siltstones or conglomerates. They contain angular to sub-angular rock and crystal fragments, reaching up to 2 cm across. Megascopically, they are massive, medium to fine grained and greyish green or purple colored rocks. Greywackes comprise crystal and lithic fragments set in a much finer clayey matrix. Crystal fragments are subsngular grains of quartz, feldspars, biotite, epidote and chlorite (Figs. 3c, d). Quartz fragments show undulose extinction, and plagioclase fragments are highly altered to sericite and kaolinite. Orthoclase and microcline occur as anhedral fragments up to 0.50 mm width and 1.00 mm length. They are usually turbid and spotted with sericite. The lithic fragments (up to 2.00 mm length) are subrounded, and intensely corroded by the clayey matrix. They mainly include trachyte, andesite, dacite, hematitized tuffs and microgranite. They are embedded together in quartz and sericite rich

matrix, sometimes with epidote, carbonates and iron oxides or ferruginous paste.

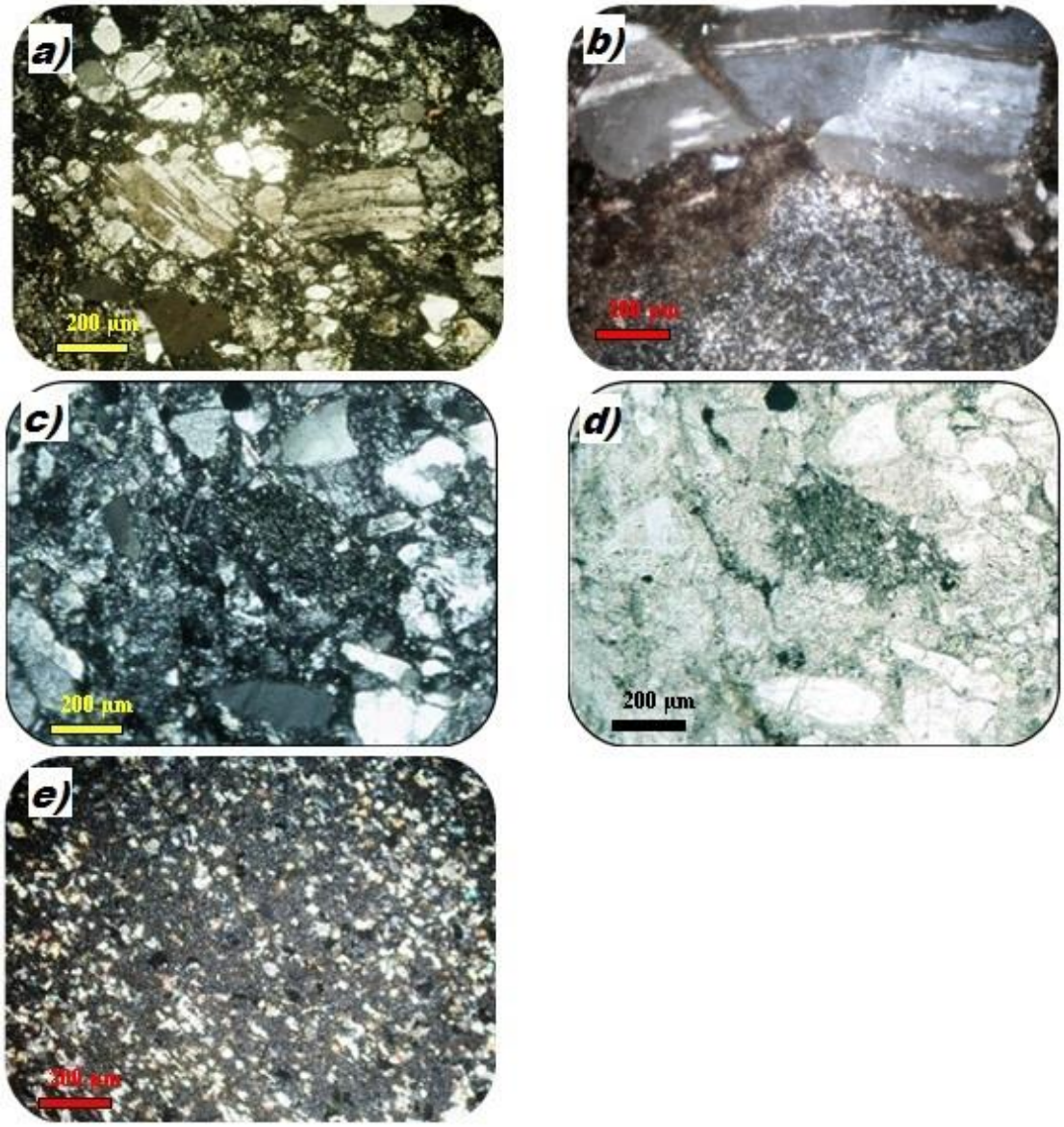

Fig 3 (a) Clasts of sandy-size quartz and plagioclase embedded in fine grained matrix in conglomerates. C.N., (b) Dislocation in a plagioclase clast together with a lithic fragment of acidic tuffs in a fine grained matrix in conglomerate. C.N., (c) Abundance angular to sub-angular clasts of quartz and highly sericitized plagioclase in fine grained matrix in greywacke. C.N., (d) The same previous view showing chlorite and the clay matrix in greywackes.P.P.L., (e) Silty sized sub-angular grains of quartz, epidote and minor feldspars with preferred orientation set in fine argillaceous matrix in siltstone. C.N.

The siltstones are less abundant than greywackes, they are mostly fine laminated grading to mudstones. Microscopically, they are essentially made up of silt-size grains (Fig 3e) of abundant quartz, thin mica flakes and with minor feldspars, chlorite, carbonate and microcrystalline volcanic rock fragment. They are set in a fine dense matrix composed of hematitic clay, argillaceous or silicic matrix. Sometimes, these banded rocks are associated with micro-faults. Quartz represents the majority of the detrital components and occurs as angular to subangular grains (up to 0.25 mm across), showing undulose extinction. Feldspar is subordinate in amount relative to quartz, and mainly represented by plagioclase which are mostly fresh with lamellar twinning and minor amounts of microcline showing different degrees of alteration. Lithic fragments are lesser than quartz and feldspar. Iron oxides occur as

fine granules associated with chlorite or coating quartz grains. Epidote predominates in the matrix and presents as fine crystal aggregates showing high interference colors.

Geochemical investigation

The Hammamat sedimentary rocks in the studied area are mainly represented by conglomerates, greywackes and siltstones. The chemical analysis for major oxides and trace elements of the studied Hammamat sedimentary rocks (four samples of siltstones, three samples of greywackes and four conglomerates) are compiled in (Tab 1).

Tab 1 *Geochemical XRF analysis and CIPW norm of Hammamat sediments in the study area*

	S1	S2	S3	S4	G10	G11	G12	C6	C7	C8	C9
	Siltstones				**Greywackes**			**Conglomerates**			
Major elements in wt%											
SiO_2	65.88	68.01	67.1	68.5	63.7	63.1	62.8	64.52	63.02	63.44	66.3
TiO_2	0.57	0.52	0.66	0.6	0.56	0.64	0.51	0.63	0.56	0.61	0.53
Al_2O_3	15.4	14.88	15.22	14.79	14.55	14.7	14.49	13.97	14.6	15.45	14.7
Fe_2O_3	1.39	1.44	1.6	1.76	2.97	3.1	3.04	1.23	1.27	1.33	1.2
FeO	3.4	3.29	2.77	3.02	0.29	0.4	0.39	2.6	3.28	3.66	3.11
MnO	0.19	0.21	0.18	0.14	0.17	0.17	0.16	0.27	0.21	0.28	0.17
MgO	1.52	1.4	1.35	1.22	1.72	1.9	1.66	1.88	2.43	2.47	1.88
CaO	2.47	2.49	2.57	2.54	4.6	4.49	4.53	2.5	3.14	3.23	2.64
Na_2O	3.25	1.85	2.02	3.5	3.48	3.7	3.6	3.4	4.15	4.13	3.87
K_2O	2.86	1.12	1.09	2.3	2.41	2.48	2.51	2.33	3.6	3.3	2.96
P_2O5	0.09	0.06	0.07	0.08	0.21	0.23	0.26	0.08	0.09	0.08	0.08
L.O.I	2.3	4.3	4.66	1.6	4.66	4.8	5.25	5.1	3.2	1.6	2.1
Total	99.32	99.57	99.29	100.05	99.32	99.71	99.2	98.51	99.55	99.58	99.54
Trace elements in ppm											
Sr	410	235	170	185	174	212	139	184	211	175	106
Rb	11	22	41	31	81	45	7	32	44	17	18
Ba	514	622	257	308	632	810	25	74	35	85	11
Ni	10.4	9.5	6.3	11	2.5	13	35	45	30	42	89
Cr	11.5	28	47	50	101	28	70	22	31	45	56
Y	18.7	23.8	19	21	19	22	29.5	7	2	6	5
Zr	70.4	158	101	88	218	315	141	66	92	112	75
Ta	-	-	2	2	1.1	4.1	1.5	2.5	3.1	2	1.6
Nb	4.1	5.2	7.8	10.19	10	12.5	4	6	5	5	8
Co	35.5	24	31.45	28.5	11.8	4	29	31	25	27	38
Pb	23.3	13.5	26.6	19	33.5	16.4	18	9.5	20.7	17	13.2
V	140	27	65	111	75	55	29	18	24	22	19
Zn	88	90	62	70	49	62	38	27	31	20	28
Cu	16.8	50	44	15.5	20	68	32	65	43	74	50.6

	S1	S2	S3	S4	G10	G11	G12	C6	C7	C8	C9
	Siltstones				**Greywackes**			**Conglomerates**			
CIPW Norm											
Quartz	26.57	43.62	42.44	30.72	23.32	21.2	21.83	26.39	13.92	14.4	22.31
Zircon	0.01	0.03	0.02	0.02	0.04	0.06	0.03	0.01	0.02	0.02	0.02
Orthoclase	16.9	6.62	6.44	13.59	14.24	14.66	14.83	13.77	21.27	19.5	17.49
Albite	27.5	15.65	17.09	29.62	29.45	31.31	30.46	28.77	35.12	34.95	32.75
Anorthite	11.9	12.16	12.4	12.2	16.96	16.18	15.97	11.95	10.58	13.87	12.61
Magnetite	2.02	2.09	2.32	2.55	0	0	0.3	1.78	1.84	1.93	1.74
Ilmenite	1.08	0.99	1.25	1.14	0.96	1.21	0.97	1.2	1.06	1.16	1.01
Apatite	0.21	0.14	0.17	0.19	0.5	0.54	0.62	0.19	0.21	0.19	0.19
Hematite	0	0	0	0	2.97	3.1	2.83	0	0	0	0
Diopside	0	0	0	0	3.49	3.75	3.78	0	3.67	1.4	0
Hyperthene	8.29	7.87	6.37	6.4	2.67	3	2.38	7.91	8.69	10.6	8.85
Olivine	0	0	0	0	0	0	0	0	0	0	0
Corundum	2.6	6.17	6.17	2.07	0	0	0	1.47	0	0	0.51

The studied rocks show a relatively wide range in SiO_2 (62.8-68.5%), Al_2O_3 (13.97-15.45 %), MgO (1.22-2.47 %), K_2O (1.05-4.4 %), L.O.I. (1.6-5.25 %), Ba (11-632 ppm) and Zr (66-315 ppm) contents revealing variable source materials (Tab 1).

Geochemical classification:

On the Log (Na_2O/K_2O) versus Log (SiO_2/Al_2O_3) variation diagram (Pettijhon et al., 1973) with boundaries redrawn by Heron (1988), all the studied samples plot in the greywacke field (Fig 4a), suggesting the same origin of the studied samples. On the Log ($Fe_2O_3^*/K_2O$) versus Log (Na_2O/K_2O) variation diagram (Heron, 1988), the most of Hammamat rock samples plot in the field of greywacke (Fig 4b), only two samples of siltstones fall in the field of Fe-shale.

Geochemical evidence of provenance:

The nature of the source of the Hammamat sedimentary rocks can be deduced from their chemical composition. A discrimination function diagram of Roser and Korsch (1988) is used to distinguish between sediments. The discriminant functions are given from the following equations:

$$F1=-1.773TiO_2+0.607Al_2O_3+0.76Fe_2O_3^*-1.5MgO+0.616CaO+0.509Na_2O-1.224K_2O-0.09$$

$$F2= 0.445TiO_2+0.07Al_2O_3-0.25Fe_2O_3^*-1.14MgO+0.438CaO+1.475Na_2O+1.426K_2O-6.861$$

According these discriminant functions (Fig. 4c), the studied samples fall within the felsic and intermediate provenance. In the terms of igneous petrology, the sources are intermediate and acidic.

Another discrimination function diagram of Roser and Korsch (1988) is used to distinguish between sediments depending on the following equations:

$$F1= 30.638\ TiO_2/Al_2O_3 -12.541\ Fe_2O_3^*/Al_2O_3+7.329\ MgO/Al_2O_3+12.031\ Na_2O/Al_2O_3 + 35.402\ K_2O/Al_2O_3 - 6.382$$

$$F2= 56.5\ TiO_2/Al_2O_3 -10.879\ Fe_2O_3^*/Al_2O_3+30.875\ MgO/Al_2O_3-5.404\ Na_2O/Al_2O_3+11.112\ K_2O/Al_2O_3 - 3.89$$

According the previous discrimination functions (Fig 4d), the studied samples fall within felsic and intermediate provenances, but three conglomerate samples fall within quartzose sedimentary provenance. Accordingly, in the terms of igneous petrology, the sources are intermediate and acidic.

Tectonic setting:

The log (K_2O/Na_2O) versus SiO_2 discrimination diagram (after Roser and Korsch, 1988) is used to outline the tectonic setting of the present study Hammamat sedimentary rocks (Fig. 4e). As shown in the figure, all samples plot within the field of active continental margin.

The discrimination function diagram (after Bhatia 1983) is used to reveal tectonic setting of sediments depending on the following equations:

$$F1= -0.0447SiO_2–0.972TiO_2+0.008Al_2O_3–0.267Fe_2O_3+0.208FeO–3.082MnO+0.14\ MgO+0.195\ CaO+0.719\ Na_2O–0.032\ K_2O+7.51P_2O_5+0.303$$

$$F2=-0.421SiO_2+1.988TiO_2–0.526Al_2O_3–0.551Fe_2O_3–1.61FeO+2.72MnO+0.881MgO–0.907\ CaO–0.177Na_2O–1.84\ K_2O+7.244\ P_2O_5+43.57$$

According the previous discrimination functions (Fig 4f), the studied samples fall within fields of active continental margin, passive margin and continental island arc.

Major element compositions are used in a ternary discriminant diagram (after Kroonenberg, 1994), the studied Hammamat sedimentary rocks plot within an overlap between active continental margin and continental arc fields (Fig 4g). Two samples of siltstone fall in the field of passive margin. Moreover, Bhatia (1983) used the major element compositions to discriminate between the oceanic island arc, continental island arc, active continental margins and passive margins tectonic environment. On the TiO_2 versus $Fe_2O_3^T$+MgO and Al_2O_3/SiO_2 versus $Fe_2O_3^T$+MgO variation diagrams (Fig 4 h-i), most of the studied samples plot within or closed to the continental island arc field.

From all above, the studied Hammamat sedimentary rocks were probably formed in a continental arc setting.

Summary and conclusion

The Hammamat sedimentary rocks or intramountaneous sediments of molasse type are represented by bedded series of conglomerates, greywackes and siltstones. The Hammamat sedimentary rocks are exposed as relatively low hills and masses compared with Gabal Kharaza Dokhan volcanics. These sedimentary rocks unconformably overlie the Dokhan volcanics and are intruded by the younger granites. They can be easily distinguished from the country rocks by their distinct bedding. Bedding is expressed in the alternation of conglomerate beds with greywacke and siltstone beds striking NE-SW. The most common alteration features in Hammamat sedimentary rocks are hematitization, kaolinization and epidotization. The microfractures of these rocks are sometimes filled with quartz and feldspar veinlets. The presence of volcanic fragments in the conglomerates indicates that these Hammamat sedimentary rocks are younger than the Dokhan volcanics. On the other hand, the Hammamat sedimentary rocks are older than the younger granites that intrude them with sharp intrusive contact. Geochemical studies revealed that the Hammamat sedimentary rocks were originated from felsic and intermediate igneous sources. Also, these rocks were probably formed in a continental arc setting.

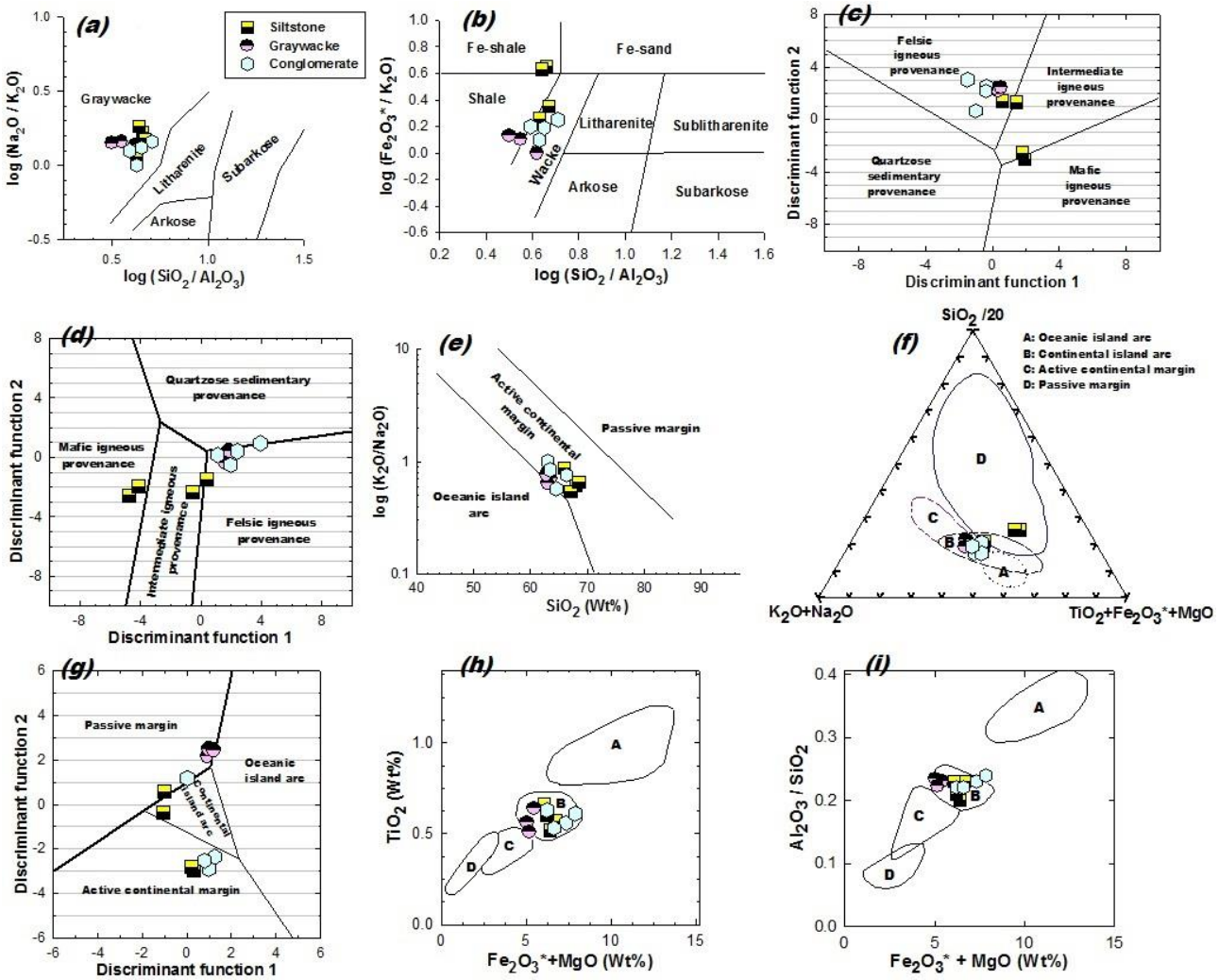

Fig 4 (a) Log (Na_2O/K_2O) versus Log (SiO_2/Al_2O_3) diagram discriminating among type of terrigenous sandstones from Pettijohn et al. (1973) with boundaries redrawn by Herron (1988), (b) Log ($Fe_2O_3^*/K_2O$) versus Log (SiO_2/Al_2O_3) diagram discriminating among type of terrigenous sandstones (Herron, 1988), (c) Discriminant Function diagram for the provenance signatures of sandstone-mudstone suites (after Roser and Korsch, 1988). Symbols are as in fig. (4a), (d) Discriminant Function diagram for the provenance signatures of sandstone- mudstone suites (after Roser and Korsch, 1988), (e): The log (K_2O/Na_2O) vs. SiO_2 discrimination diagram (after Roser and Korsch, 1988) for the studied Hammamat sedimentary rocks. Symbols are as in fig. (4a), (f): Discrimination function diagram (after Bhatia, 1983) for the studied Hammamat sedimentary rocks, (g): Plot of the major element composition of the studied Hammamat sedimentary rocks on the tectonic setting discrimination diagram (Kroonenberg, 1994), (h-i): Discrimination diagrams for the studied Hammamat sedimentary rocks (after Bhatia, 1983), based upon (h) a bivariate plot of TiO_2 vs. (Fe_2O_3*+MgO) and (i) a bivariate plot of Al_2O_3/SiO2 vs. (Fe_2O_3*+MgO). Field labels as in Fig.-(4.g) and symbols as in Fig. (4a)

References

Akaad, M. K., and Noweir, A. M., 1980. Geology and lithostratigraphy of the Arabian Desert orogenic belt of Egypt between lat. 25o 35` and 26o 30` N. Inst. *App. Geol., Jeddah,* Bull. 3. V. 4, pp. 127 - 135.

Bhatia, M. R., 1983. Plate tectonics and Geochemical compoisition of sandstones. J. *Geol*., V. 91, No. 6, pp. 611-627.

El Gaby, S., List, F., Tehrani, R., 1990. The basement complex of the Eastern Desert and Sinai. In *The Geology of Egypt*. Said, R. (Ed.), Rotterdam, Balkema, pp. 175–184.

El Kalioubi, B.A., 1996. *Provenance, tectonic setting and geochemical characteristics of the Hammamat molasses sediments around Umm had pluton, Eastern Desert, Egypt*. MERC, Ain Shams Univ., Earth Sci. Ser. 10, 75–88.

Hassan, M.A., Hashad, A.H., 1990. Precambrian of Egypt. In: *Said, R. (Ed.), The Geology of Egypt*. Balkema, Rotterdam, pp. 201–248.

Herron, M.M., 1988. Geochemical classification of terrigenous sands and shales from core or log data. *J. Sed. Petrol.*, V. 58, pp. 820-829.

Kroonenberg, S.B., 1994. Effects of provenance, sorting and weathering on the geochemistry of fluvial sands from different tectonic and climatic environments. In *Proceedings of the 29th International Geological Congress*, Part A, p. 69–81.

Pettijohn, F. J., Potter, P. E. and Silver, R., 1973. *Sand and siltstone*. New York : Springer-Verlag, 618 p.

Roser, B. P. and Korsch, R. J., 1988. Provenance signatures of sandstone-mudstone suited determined using discriminant function analysis of major element data. *Chem. Geol*. V. 67, pp. 119-139.

Stern, R. J. and Hedge, C. E., 1985. Geochronologic and isotopic constraints on late Precambrian crustal evolution in the Eastern Desert of Egypt. *Amer. J. Sci.*, V.258, p. 97-127.

Shalaby, A., Stüwe, K., Fritz, H., Makroum, F., 2006. The El Mayah molasse basin in the Eastern Desert of Egypt. *Journal of African Earth Sciences*, 45, 1–15.

Shapiro, L., Brannock, W.W., 1962. Rapid analysis of silicate, carbonate and phosphate rocks. *U. S. Geol. Surv. Bull.*, V. 1144-A, P. 1-56.

Willis, K.M., Stern, R.J. & Clauer, N., 1988. Age and geochemistry of Late Precambrian sediments of the Hammamat Series from the Northeastern Desert of Egypt. *Precambrian Research*, 42, 173–187.